Mausam, (1988), **39**, 2, 139-148

551.509.313(213)

A suitable scheme of dynamic initialization for a multi-level primitive equations model in tropics

U. C. MOHANTY, R. K. PALIWAL*, A. TYAGI*, S. C. MADAN and V. B. SARIN

Centre for Atmospheric Sciences, I.I.T., New Delhi

(*Received 17 February 1987*)

सार — उष्णकटिबन्धीय क्षेत्रों के लिए उपयुक्त गतिकीय प्रारम्भीकरण प्रक्रिया का पता लगाने के लिए कई आंकिक प्रयोग किए गए हैं। ये प्रयोग बहुस्तरीय सिगमा ऊर्ध्वाधर निर्देशांक मानकर पूर्वग समीकरण प्रतिदर्श के साथ किए गए हैं। विभिन्न गतिकीय प्रारम्भीकरण प्रक्रियाओं की कार्य-कुशलता की प्रारम्भिक 12 व 24 घण्टों के पूर्वानुमान क्षेत्रों से परख की गई है। इससे पाया गया है कि यद्यपि विभिन्न गतिकीय प्रारम्भीकरण प्रक्रियाएं सामान्यतः समान परिणाम प्रदान करती हैं किन्तु सम्पूर्ण कार्य-कुशलता तथा संगणक (कम्प्यूटर) समय की बचत को दृष्टि में रखते हुए ओकामुरा प्रक्रिया उपयुक्त पाई गई है।

ABSTRACT. A number of numerical experiments are carried out to find a suitable dynamic initialization scheme for tropics. The experiments are carried out with a multi-level primitive equations model with sigma as the vertical coordinate. The performance of different initialization schemes are evaluated from the initialized and 12 and 24 hours forecast fields. It is found that all the different types of dynamic initialization yield almost similar results. However, on the basis of the overall performance and computational economy considerations, the Okamura scheme is preferred.

1. Introduction

It has been widely demonstrated that the short range (6 hr to 48 hr) numerical weather prediction based on limited area primitive equation (PE) model is very much sensitive to the initial data and boundary conditions. Integration of such a model with the initial state of atmosphere requires a mutually balanced mass and velocity fields and appropriate boundary conditions. Otherwise, unrealistic, unwanted high frequency gravity waves, called as 'meteorological noise', are amplified during the process of integration of the model. A number of numerical techniques called as 'initialization' have been developed to overcome the problem by achieving a balance between mass and velocity fields. There are three basic approaches to the problem of initialization, *viz.*, static, dynamic and normal mode initialization. A detailed review of these schemes are given by Bengtsson (1975), Daley (1981), Sugi (1986) and many others.

Though the normal mode initialization (NMI) is found to be more suitable for a global PE model, its application for limited area PE models is very much restricted. Briere (1982), Bourke and McGregor (1983), showed the use of NMI for limited area models. However, all these studies are confined to mid-latitudes and the application of NMI to limited area models (LAM) in equatorial tropical region is yet to be fully resolved. The gravitational noise control mechanism in dynamic initialization (DI) is the numerical viscosity which is created by Euler backward (EB) scheme during forward and backward time integration of the model. This scheme is widely used in LAM (PE) of the tropics, *viz.*, Krishnamurti *et al.* (1973), Das & Bedi (1978), Mohanty (1985), Singh(1985). This scheme is very simple for its adaptation in a PE model and it also gives quite reasonable results. A major disadvantage of this scheme is that it takes too much of computational time (about one day's forward integration of the model). During the last decade, a number of attempts have been made to modify the DI scheme to minimise the computational requirements for its effective operational use.

In this study, an attempt is made to examine the performance of some of the modified DI schemes for tropics. A multi-level LAM (PE) is used for this purpose.

A brief description of the model with boundary condition and finite difference scheme is given in section 2. Section 3 describes three well known approaches of DI. Inter-comparison of different DI schemes are described in section 4. Summary and conclusions are given in section 5.

2. Description of the model

All the DI experiments were carried out with a multi-level LAM (PE) for tropics (adapted from Naval Research Laboratory, U.S.A.). The horizontal domain of the model extends from 7.5°S to 45° N and 30° E to 105°E

*Directorate of Meteorology, Air Headquarters, Vayu Bhavan, New Delhi-110011.

with a grid distance of 2.5° Lat./Long. In the vertical the model has five sigma (σ) levels with $\sigma=0$ as the top and $\sigma=1$ as the bottom boundary. In the horizontal, the model variables are defined at staggered grid points using Arakawa C-grid (Arakawa and Lamb 1977). The orography is derived from US Navy data provided by NCAR and interpolated to the model grid points.

2.1. *Model equations*

The primitive equations in spherical co-ordinate governing the motion of the atmosphere appropriate to a meso-scale quasi-hydrostatic, baroclinic system with sigma ($\sigma=p/p_s$) as the vertical coordinate is formulated in flux form. The model with seven equations (five prognostic and two diagnostic) include u and v momentum equations, the thermodynamic, the moisture continuity, the surface pressure tendency, the hydrostatic and the continuity equations for the seven meteorological variables (u, v, T, q, p_s, ϕ and $\dot{\sigma}$) forms a closed system as given below :

$$\frac{\partial}{\partial t}(p_s u) + \frac{1}{h_x h_y}\left[\frac{\partial}{\partial x}(p_s u h_y u) + \frac{\partial}{\partial y}(p_s v h_x u)\right] + \frac{\partial}{\partial \sigma}(p_s \dot{\sigma} u) - f p_s v + \frac{p_s u v}{h_x h_y}\frac{\partial}{\partial y} h_x = -\frac{p_s}{h_x}\frac{\partial \phi}{\partial x} - \frac{RT}{h_x}\frac{\partial p_s}{\partial x} + p_s F_u \tag{1}$$

$$\frac{\partial}{\partial t}(p_s v) + \frac{1}{h_x h_y}\left[\frac{\partial}{\partial x}(p_s u h_y v) + \frac{\partial}{\partial y}(p_s v h_x v)\right] + \frac{\partial}{\partial \sigma}(p_s \dot{\sigma} v) + f p_s u - \frac{p_s v^2}{h_x h_y}\frac{\partial}{\partial y} h_x = -\frac{p_s}{h_y}\frac{\partial \phi}{\partial y} - \frac{RT}{h_y}\frac{\partial p_s}{\partial y} + p_s F_v \tag{2}$$

$$\frac{\partial}{\partial t}(p_s T) + \frac{1}{h_x h_y}\left[\frac{\partial}{\partial x}(p_s u h_y T) + \frac{\partial}{\partial y}(p_s v h_x T)\right] + \left(\frac{\sigma}{\sigma_0}\right)^{\kappa}\frac{\partial}{\partial \sigma}(p_s \dot{\sigma}\theta) - \frac{RT}{c_p}\widetilde{D} - \frac{RT}{c_p}\left(\frac{u}{h_x}\frac{\partial p_s}{\partial x} + \frac{v}{h_y}\frac{\partial p_s}{\partial y}\right) = p_s H_T + p_s F_T \tag{3}$$

$$\frac{\partial}{\partial t}(p_s q) + \frac{1}{h_x h_y}\left[\frac{\partial}{\partial x}(p_s u h_y q) + \frac{\partial}{\partial y}(p_s v h_x q)\right] + \frac{\partial}{\partial \sigma}(p_s \dot{\sigma} q) = p_s H_q + p_s F_q \tag{4}$$

$$\frac{\partial p_s}{\partial t} = -\widetilde{D} \tag{5}$$

$$\frac{\partial \phi}{\partial \sigma} = -\frac{RT}{\sigma} \tag{6}$$

$$\frac{\partial (p_s \dot{\sigma})}{\partial \sigma} = \widetilde{D} - D \tag{7}$$

Here, f is the coriolis parameter, u the zonal wind component, v the meridional wind component, ϕ the geopotential, T the temperature, p_s the surface pressure, q the specific humidity, $\dot{\sigma}$ the vertical velocity in σ co-ordinate, R the gas constant for dry air, θ the potential temperature, $\kappa=R/c_p$, c_p the specific heat capacity of dry air at constant pressure, D the divergence and $\widetilde{D}$ the vertically integrated horizontal and mass divergence. The vertical friction terms which include surface fluxes, vertical and horizontal diffusion of momentum, heat and moisture are represented by F_u, F_v, F_T and F_q respectively. Further, the heat and moisture source/sink are represented by H_T and H_q respectively.

2.2. *Lateral boundary conditions*

The values of u, v, T and p_s at the lateral boundaries are obtained by linear interpolation using the values at the interior two grid points, whereas constant inflow conditions have been used for the specific humidity, q, *viz.*, $\frac{\partial q}{\partial x}=q(N-1)-q(N)=0$. In addition, no flux condition has been imposed for the normal components of the wind to ensure mass conservance. The model also includes enhanced filtering near the lateral boundaries by incorporating sponge boundary conditions.

2.3. *Finite difference and time integration schemes*

The model equations are approximated by a second order accurate quadratic conserving finite difference scheme over a staggered horizontal grid system as shown in Fig. 1. Horizontal finite difference is carried out by using Arakawa C-grid (Arakawa and Lamb 1977) which is found to be a suitable scheme for simulating geostrophic adjustment in the wind field and conservance of the integral properties. Temperature (T), geopotential (ϕ), specific humidity (q) and $\dot{\sigma}$ are computed at the mass points (i, j) while east-west zonal wind (u) is computed at the mid-point of mass points along the x-axis. The north-south meridional component (v) is computed at the mid-points along the y-axis (Fig. 1).

An explicit time integration scheme is used for forecasting the prognostic variables in the Eqns. (1)-(5). First time step is carried out by Euler-backward scheme and subsequent integration steps by the Leap-frog method. The forward and backward time integration

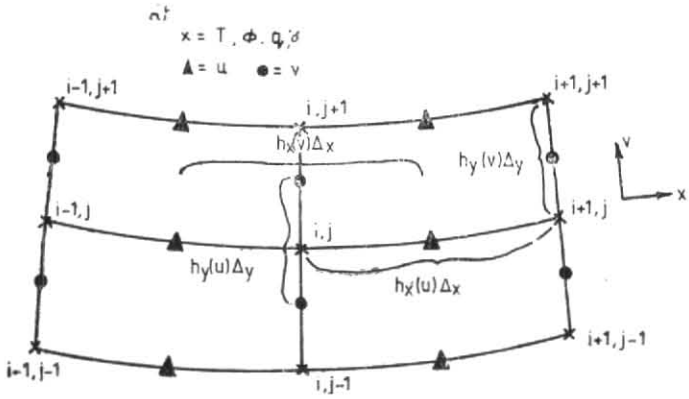

Fig. 1. Horizontal grid system (Arakawa-C)

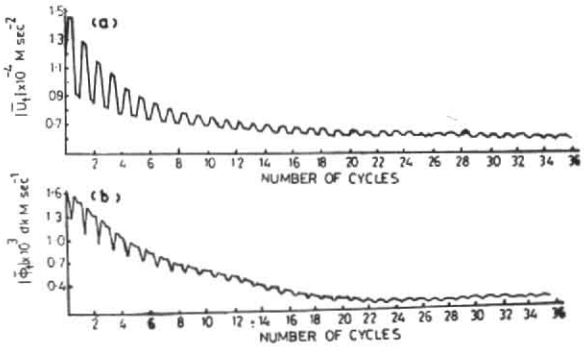

Fig. 2. Change in every step of pseudo-forecasting : (a) $|\bar{U}_t|$ and (b) $|\bar{\phi}_t|$

during the process of DI are described in detail in section 3.

2.4. *Physical processes*

In order to take into account sub-grid scale processes relevant to short range prediction, following physical processes are parameterized in the model :

(*i*) The planetary boundary layer is parameterized to include the effect of friction, vertical exchange and diffusion of heat, moisture and momentum by using bulk aerodynamic formulations.

(*ii*) The cumulus convection scheme used in the model is a slightly altered version of the scheme proposed by Kuo (1974) and subsequently modified by Anthes (1977).

(*iii*) In order to consider the unresolved horizontal scales of motion, a linear fourth order horizontal diffusion scheme is used for momentum, heat and moisture in the respective equations.

However, during the process of initialization, the physical processes were turned off.

3. Methods of dynamic initialization

A brief description of the three types of DI used in this study is given below.

3.1. *Method I*

This method is based on a four-step scheme of Matsuno (1966), comprising of a forward forecasting followed by a backward forecasting which is called as 'pseudo forecasting'. For both forward and backward time integration of the complete system of prognostic primitive Eqns. (1)-(5) except the moisture continuity equation (Eqn. 4), Euler backward scheme is used. This well known two step time integration scheme has the properties to simulate a computational viscous effect of selective damping of high frequency waves. This scheme is widely used in DI (Nitta and Hovermale 1969, Kibganov and Mohanty 1979, Mohanty and Madan 1982 and others).

For a given system of eqn. $\frac{\partial Z}{\partial t}=F(Z)$, where $Z=\begin{vmatrix} u \\ v \\ T \\ p_s \end{vmatrix}$

the four steps of dynamic initialization are :

Forward forecast

$$Z^{*}_{n+1} = Z^{v}_{n} + \Delta t . F\,(Z^{v}_{n})$$

$$Z^{v}_{n+1} = Z^{v}_{n} + \Delta t . F\,(Z^{*}_{n+1})$$

Backward forecast

$$Z^{*}_{n} = Z^{v}_{n+1} - \Delta t . F\,(Z^{v}_{n+1})$$

$$Z^{v+1}_{n} = Z^{v}_{n+1} - \Delta t . F\,(Z^{*}_{n})$$

where,

Z_n^* and Z_{n+1}^* — intermediate values of Z at the time steps n and $n+1$ respectively

Δt — time interval

v — number of iterations (No. of cycle of pseudo forecasting)

In this method, either the mass or momentum field or both the fields can be allowed to adjust during the process of initialization. However, it was found that for the tropics, a mutual adjustment process is more effective (Kibganov and Mohanty 1979). Such a mutual adjustment process is used in this study. The amplitude response of this method is $R=1-\omega^2\Delta t^2+\omega^4\Delta t^4$ where ω is the angular frequency for an oscillatory equation $Z=Z_0\, e^{i\omega t}$.

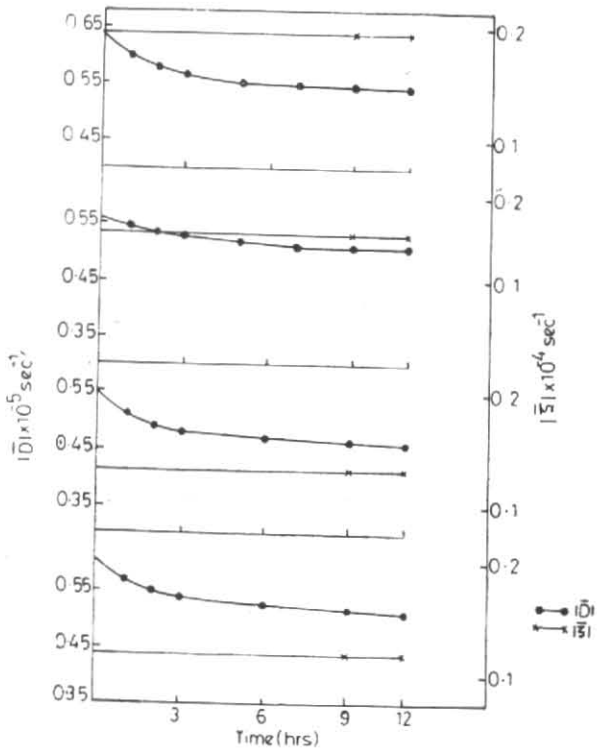

Fig. 3. Change of $|\bar{D}|$ and $|\bar{\zeta}|$ in the process of dynamic initialization

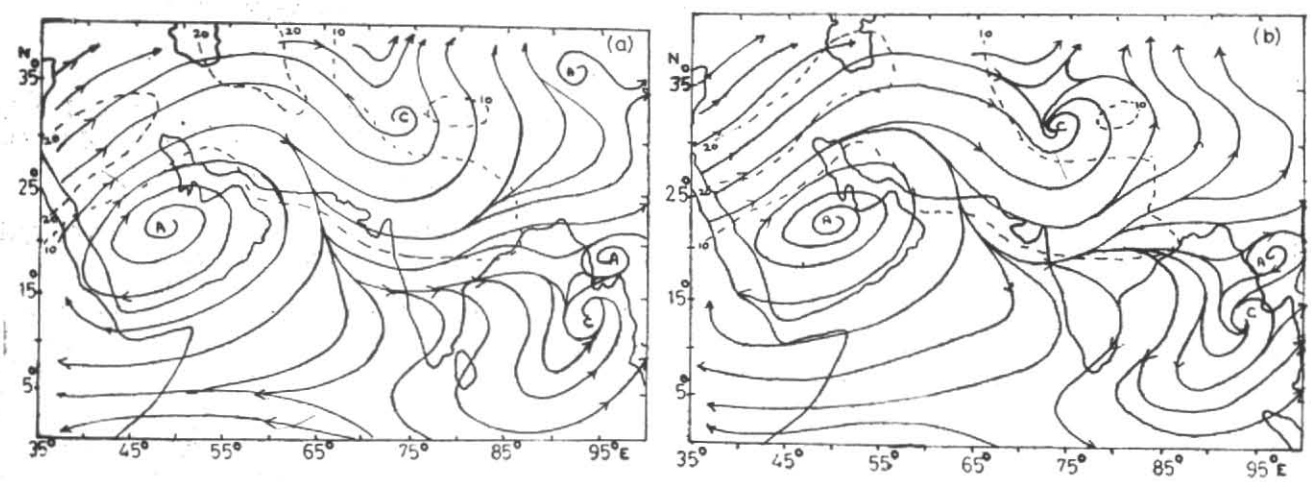

Fig. 4. Streamline isotach analysis of wind field at 500 mb for 12 GMT, 22 May 1979 : (a) uninitialized and (b) initialized

3.2. *Method II*

This method consists of three steps, a forward step and a backward step followed by an averaging. For both forward and backward integration, a simple Euler's scheme is used. This DI scheme was proposed by Okamura (Nitta 1969). This procedure of DI provides a much stronger damping as it simulates the computational viscous effect which is two times higher than the Method I. This method is also widely used for DI (Temperton 1976, Singh 1985, Sugi 1986 and others). The three steps of this type of DI are as follows :

$$Z^{*}_{n+1} = Z^{v}_{n} + \triangle t.F(Z^{v}_{n})$$

$$Z^{**}_{n} = Z^{*}_{n+1} - \triangle t.F(Z^{*}_{n+1})$$

$$Z^{v+1}_{n+1} = 3Z_{n} - 2Z^{**}_{n}$$

The amplitude response function of this scheme is

$$R = 1-2(\omega\triangle t)^2$$

3.3. *Method III*

This method of DI is similar to the Method I. However, the time integration scheme of the Method I (EB) is replaced by a modified EB scheme comprising of three steps (Kurihara and Tripoli 1976). Thus, time integration scheme is found to generate stronger damping effect than that of the normal EB scheme. In this time integration scheme, the first two steps are similar to EB scheme. In the third step, an averaging of the intermediate values of the first two steps is carried out with a weighting factor α. In case of $\alpha=0$, this scheme reduces to a normal EB method. The various steps of this type of DI are :

Forward step

$$Z^{*}_{n+1} = Z^{v}_{n} + \triangle t.F(Z^{v}_{n})$$

$$Z^{**}_{n+1} = Z^{v}_{n} + \triangle t.F(Z^{*}_{n+1})$$

$$Z^{v}_{n+1} = (1+\alpha)Z^{**}_{n+1} - \alpha Z^{*}_{n+1}$$

Backward step

$$Z^{*}_{n} = Z^{v}_{n+1} - \triangle t.F(Z^{v}_{n+1})$$

$$Z^{**}_{n} = Z^{v}_{n+1} - \triangle t.F(Z^{*}_{n})$$

$$Z^{v+1}_{n+1} = (1+\alpha)Z^{**}_{n} - \alpha Z^{*}_{n}$$

where α is a weight factor which controls the strength of damping. The amplitude response of this method is $R=1-(2\alpha+1)\omega^2(\triangle t)^2+(1+\alpha)^2\,\omega^4(\triangle t)^4$. This method of DI is used by Dey (1979). In this method, by prescribing a suitable value of α, it is possible to vary the magnitude of computational viscosity for the selective damping of high frequency waves. In this study, value of α has been taken as 1 and 3 and like the other two methods, mutual adjustment of mass and velocity fields is allowed.

4. Results of numerical experiments

All the numerical experiments on initialization and forecasting were carried out with a five-level PE model described in section 2. The data used for these experiments is the First GARP Global Experiment (FGGE) level IIIb analysis for 12 GMT of 22 May 1979 produced by the European Centre for Medium Range Weather Forecasts (ECMWF).

The results on characteristics of DI, inter-comparison of the three different types of DI and impact of initialization on the forecast are discussed in the following three sub-sections.

4.1. *Characteristics of dynamic initialization*

The results of characteristics of initialization are presented for Method I. In order to examine the role of initialization in simulation of computational viscosity at the end of each of the four steps of the pseudo-forecasting, we have calculated :

$$|\bar{Z}_{t}| = \frac{1}{(M-2)(N-2)}\sum_{i=2}^{N-1}\sum_{j=2}^{M-1}\frac{|Z_{n+1}-Z_{n}|}{\triangle t}$$

The values of $|\bar{U}_t|$ and $|\bar{\phi}_t|$ at $\sigma=0.5$ are illustrated in Figs. 2(a) and 2(b) respectively. It is observed from Fig. 2 that during first one or two hours of initialization, damping was quite intense and afterwards become negligible. Further, it is found that the mass and velocity fields have undergone damping with an opposite phase which explains the mechanism of mutual adjustment during the process of initialization.

To demonstrate the properties of DI to provide selective filteration of only high frequency gravity modes without affecting the large scale motion of the atmosphere, the level average vorticity and divergence are presented for four different sigma surfaces ($\sigma=0.9$, 0.7, 0.5 and 0.3) in Fig. 3. While in the process of initialization, mean vorticity ($|\bar{\zeta}|$) remained almost constant, strong damping of mean divergence ($|\bar{D}|$) was observed at each of the levels. This damping is strongest at $\sigma=0.3$ and least at $\sigma=0.5$ (equivalent to 300 and 500 mb levels respectively). These results are similar to the one reported by Mohanty (1982) for a barotropic PE model.

During the process of initialization, velocity and mass fields characterising the synoptic and large scale features of the atmosphere remain unchanged. For an example, the flow pattern at 500 mb level before initialization and after 12 hours of initialization by Method II are illustrated in Fig. 4. As it is seen from Fig. 4 that the location and circulation patterns of all the synoptic systems remain unchanged. However, slight weakening of cyclonic and anticyclonic systems are reflected in geopotential fields (figures not presented).

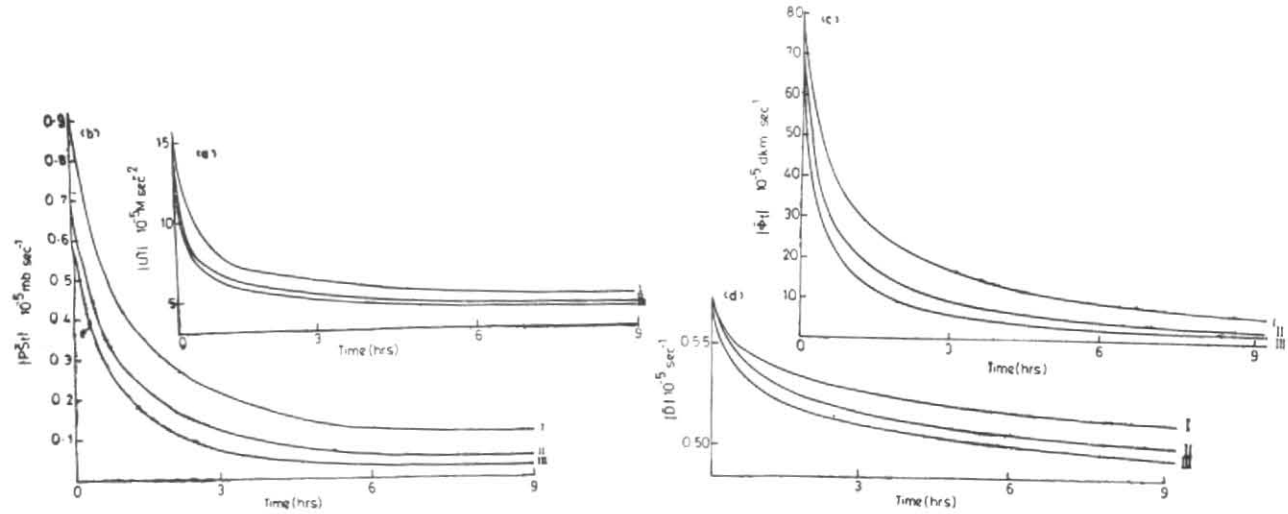

Fig. 5. Change in the process of dynamic initialization (Methods I, II and III) : (a) $|\bar{U}_t|$, (b) $|\bar{p}_{st}|$, (c) $|\bar{\phi}_t|$ and (d) $|\bar{D}|$

TABLE 1

RMSE values between the initial and initialized fields by the three different methods

level (mb)	RMSE 'u' (m/sec) Method			RMSE 'v' (m/sec) Method			RMSE 'T' (°C) Method		
	I	II	III	I	II	III	I	II	III
200	0.82	0.70	0.79	0.72	0.69	0.70	0.19	0.17	0.18
300	0.63	0.54	0.65	0.53	0.51	0.56	0.19	0.17	0.18
500	0.54	0.53	0.57	0.41	0.41	0.43	0.18	0.17	0.19
700	0.44	0.42	0.46	0.33	0.32	0.34	0.19	0.18	0.20
850	0.38	0.29	0.38	0.29	0.27	0.29	0.20	0.19	0.19

4.2. *Inter-comparison of initialization schemes*

The results of performance of three different initialization schemes, described in section 3, are demonstrated here.

For this purpose, the absolute mean of $|\bar{U}_t|$, $|\bar{\phi}_t|$, $|\bar{D}|$ for the mid-level ($\sigma=0.5$) and $|\bar{p}_{st}|$ at the end of each cycle during the process of initialization by three different methods are presented in Fig. 5. It is found that the damping is very intensive for all these parameters during the first three hours of pseudo-forecasting. After a period of 5 to 7 hours of initialization, damping of all these parameters become negligible. Maximum reduction in the amplitude is observed in the case of $|\bar{p}_{st}|$ and $|\bar{\phi}_t|$.

The nature of damping in the process of DI by all the three methods is found to be similar. However, the rate of damping is more intensive by Method III and least by Method I which agrees very well with the theoretical values of amplitude response (R) of these methods. For example, the reduction in the magnitude of $|\bar{U}_t|$ become negligible after three hours of pseudo-forecasting by Method III while Method I and Method II take 7 and 4 hours respectively. Almost similar behaviour is observed in the case of other parameters. However, this does not provide a clear indication of the superiority of one method over others. Since it is observed that even after 9 hr of initialisation when the changes in all the fields become almost negligible, the magnitude of $|\bar{U}_t|$, $|\bar{\phi}_t|$, $|\bar{p}_{st}|$ and $|\bar{D}|$ are found to be least in case of Method III and maixmum in the case of Method I. By introducing a maixmum computational viscosity in Method III and least in Method I, there may be undesirable damping of essential meteorological informations to some extent during the process of DI.

Assuming that the initial fields before initialization are in a reasonable state of balance and true representative of the real atmosphere, an attempt is made to evaluate the changes in the values of mass and velocity fields due to different types of DI. For this purpose root mean square error (RMSE) of the 12 hours initialized zonal and meridional wind components and temperature with respect to the corresponding initial fields are evaluated and presented in Table 1 It is seen from Table 1 that the RMSE values for the three

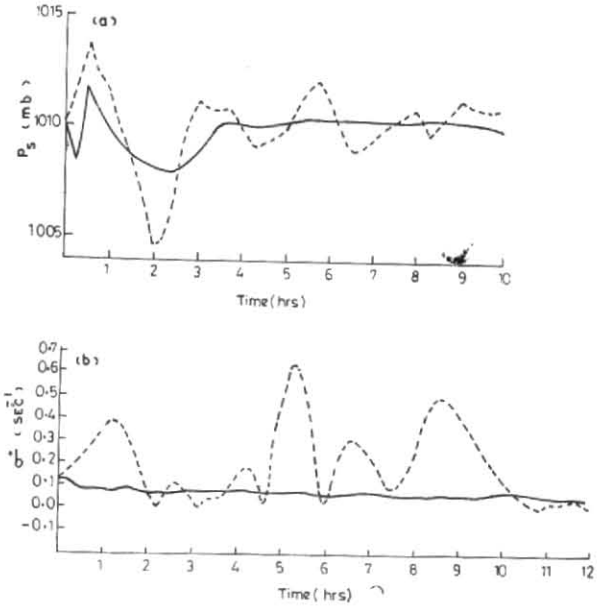

Fig. 6. Time-series at the location (65°E, 30°N) of : (a) surface pressure p_s (in mb) and (b) vertical velocity ($\dot{\sigma}$) in sec^{-1} at $\sigma = 0.5$ (approx. 500 mb) during one day forecast. Dashed line for the forecast from uninitialized data and solid line for the forecast from initialized data (Method II)

TABLE 2

RMSE of 12-hour forecast obtained from different types of initialized input

Level (mb)	RMSE 'u' (m/sec)				RMSE 'v' (m/sec)				RMSE 'T' (deg. C)			
	No initialization	Method I	Method II	Method III	No initialization	Method I	Method II	Method III	No initialization	Method I	Method II	Method III
200	5.48	4.11	3.61	4.25	6.04	5.35	4.91	5.28	2.57	1.91	0.98	1.86
300	4.65	4.15	4.07	4.15	5.01	4.95	4.32	4.69	2.47	1.88	1.75	1.83
500	3.90	3.0	2.31	2.96	3.52	3.50	2.16	2.26	1.90	1.36	1.26	1.28
700	3.58	2.52	2.47	2.89	3.63	3.56	2.60	2.62	1.43	1.33	1.28	1.37
850	4.02	2.87	2.51	2.56	2.51	2.23	2.07	2.21	1.73	1.54	1.35	1.46

different methods are not significantly different. However, in most of the cases, the RMSE is least for Method II and maximum for Method III.

From these inter-comparisons, it is obvious that the performance of all the three methods are almost similar. However, from the point of view of computational requirements for the different initialization methods it is evident that Method II is more economical as compared to the other two methods (*e.g.*, Method III requires double the time for computations as compared to Method II).

From the dynamic initialization point of view, it is obvious that Method II is more desirable from performance and computational economy considerations.

4.3. *Impact of initialization on short-range* (12-24 *hours*) *forecasting*

Fig. 6 shows the time plots of the surface pressure (p_s) and vertical velocity ($\dot{\sigma}$) in sigma co-ordinate for the level $\sigma = 0.5$ at a specific location (30° N, 65° E) during a one day forecast produced without initialization (dashed line) and with 12 hours of initialization by

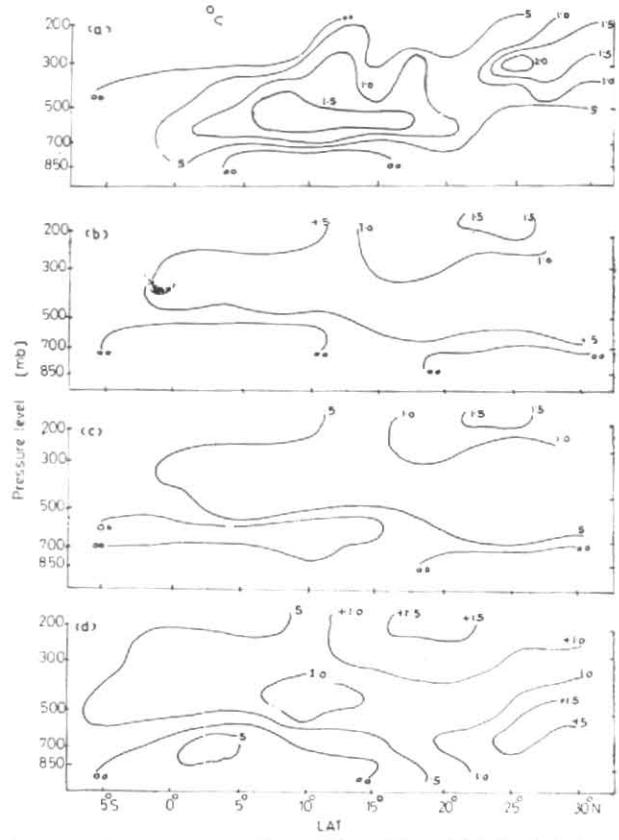

Fig. 7. The zonal average 12 hours forecast error of T with : (a) uninitialized data and with initialised data by : (b) Method I, (c) Method II and (d) Method III

Method II (solid line). Spurious fluctuations in the p_s and $\dot{\sigma}$ fields which appear during the model time integration without initialization are clearly suppressed in the model run started with the initialized fields.

Root mean square error of temperature, zonal and meridional components of wind for 12 hours integration of the model with respect to the corresponding verification fields over an interior region bounded by 5 °S-30° N and 45° E-95° E are given in Table 2.

It is obvious to see from this table that at all the five levels RMSE for u, v and T are maximum with uninitialized data as the initial state for the model. It may be noted that the RMSE of u, v and T fields obtained after 12 hours of forecast run from the three different initialized input fields are almost similar, though in all the cases, Method II results are better than others.

The zonal average 12 hours forecast error of temperature with uninitialized and initialized fields (by three different methods) are illustrated in Fig. 7. The forecast error obtained from the uninitialized data is quite large compared to those from initialized input fields. It is seen that the results from the initialised fields obtained from Methods I and II are least and almost identical. Similar type of results are obtained in respect of other variables. Even the geographical distribution of u, v and T give the similar type of results (figures not presented). This again confirms that the initialization by Method II gives a better forecast than the other two methods, though the differences are not so significant.

Fig. 8 depicts flow-pattern at 500 mb of model forecast for 12 hours with initialised (Method II) and uninitialized input fields along with the corresponding observed analysis. It is seen from Fig. 8, that the location and intensity of the mid-tropospheric trough in westerlies over northern India together with the anticyclonic circulations over Arabia and Burma are well predicted by the model forecast obtained with the initialized input data. Similarly, the cyclonic circulation over north Andman Sea is also well brought out. On the other hand, the forecast obtained with uninitialized input data distorts the location and intensity of the trough and of the two anticyclonic circulations over Arabia and Burma. Moreover, in this forecast the north Andman Sea cyclonic circulation is wiped out and spurious anticyclonic circulations are created over Bay of Bengal & China. The flow patterns predicted with initialized data obtained from Methods I and III are very much similar to that from Method II and, therefore, the results are not presented. This clearly demonstrates the need for initialized fields as input data for the model integration.

5. Conclusion

On the basis of the above stated results, we can make the following concluding remarks:

(*i*) The dynamic initialization exhibits the property of selective filteration of high frequency wave spectrum. Further, this initialization does not significantly alter the broad features of large scale processes and the centres of atmospheric vortices.

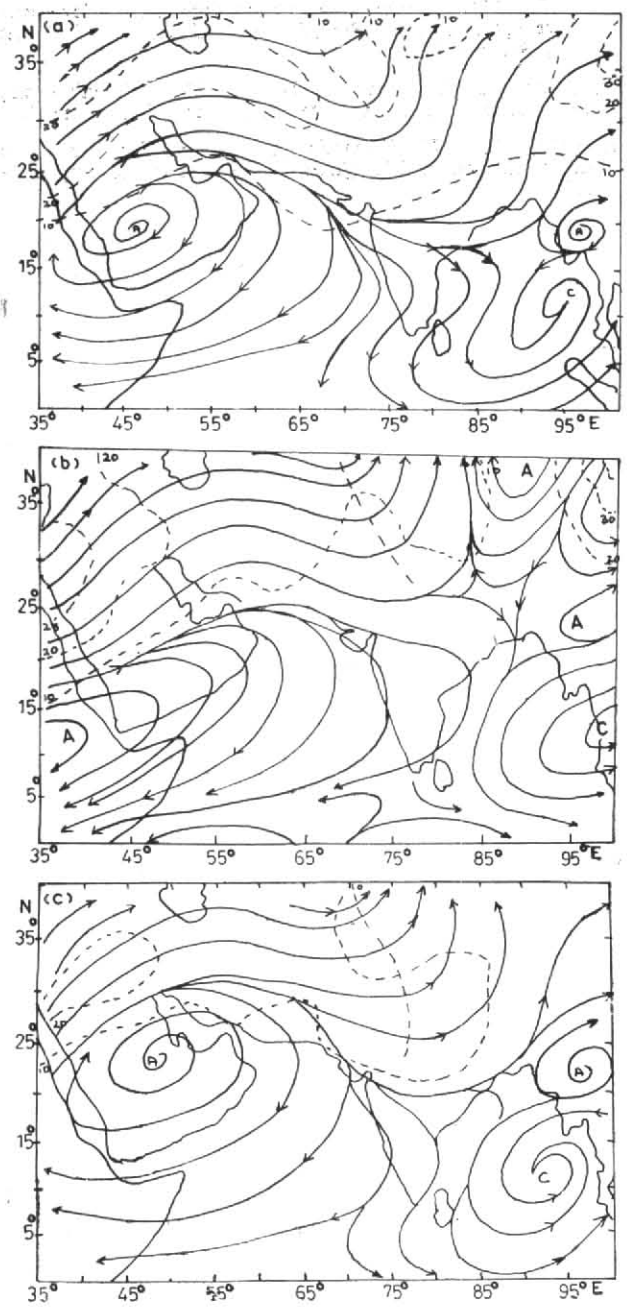

Fig. 8. Stream-line isotach analysis of wind field at 500 mb of 12 hours forecast obtained from : (a) initialized data, (b) uninitialized data of 22 May 1979 (12 GMT) and (c) of the corresponding observed field at 23 May 1979 (00 GMT)

(*ii*) The performance of three different types of dynamic initialization schemes, yield almost similar type of results, both qualitatively as well as quantitatively. Further, no significant differences are observed even in the 12 hours forecast fields obtained from the different initialized fields. However, from the point of view of computational economy and performance, Method II, *viz.*, Okamura method (Nitta 1969), is more acceptable.

(*iii*) For initialization of a multi-level PE model in tropics with wind field as one of the input data, dynamic initialization is very much essential as without such an initialization, a large forecast error is observed in short range weather forecasts (12-24 hours).

Acknowledgements

The authors express their gratitude to Prof. P.K. Das for encouragement, kind interest and many useful discussions, to Prof. M.P. Singh, Head, Centre for Atmospheric Sciences for the keen interest, and Mr. K.J. Ramesh for their computational help.

References

Anthes, R.A., 1977, A cumulus parameterization scheme utilizing a one-dimensional cloud model, *Mon. Weath. Rev.*, **105**, pp. 280-286.

Arakawa, A. and Lamb, V.R., 1977, Computational design of the basic dynamical process of the ULCA General Circulation Model, *Methods in Computational Physics*, **17**, pp. 174-265.

Bengtsson, L., 1975, *4-dimensional assimilation of meteorological observations*, GARP Publications Series No. 15, 76 pp.

Bourke, W. and McGregor, J.L., 1983, A non-linear vertical mode initialization scheme for a limited area prediction model, *Mon. Weath. Rev.*, **111**, pp. 2285-2297.

Briere, S., 1982, Nonlinear normed mode initialization of a limited area model, *Mon. Weath. Rev.*, **110**, pp. 1166-1186.

Daley, R., 1981, Normal mode initialization, *Rev. Geophys. Space Phys.*, **19**, pp. 450-468.

Das, P.K. and Bedi, H.S., 1978, The inclusion of Himalayas in a primitive equation model, *Indian J. Met. Hydol. Grophys.*, **29**, pp. 375-383.

Dey, C., 1979, An integration technique especially efficient in Dynamic Initialization, *Mon. Weath. Rev.*, **107**, pp. 1287-1298.

Kibganov, A.F. and Mohanty, U.C., 1979, On the dynamic initialization of wind and geopotential fields in the low latitudes, *Met. & Hydrol.*, **8**, 40-48.

Krishnamurti, T.N., Kanamitsu, M., Ceselski, B. and Mathur, M.B., 1973, Florida State University's Tropical Prediction Model, *Tellus*, **25**, pp. 523-535.

Kuo, H.L., 1974, Further studies of the parameterization of the influence of cumulus convection on large scale flow, *J. atmos. Sci.*, **31**, pp. 1232-1240.

Kurihara, Y. and Tripoli, G.J., 1976, An iterative time integration scheme designed to preserve a low-frequency wave, *Mon. Weath. Rev.*, **104**, pp. 761-764.

Matsuno, T., 1966, Numerical integration of the primitive equations by a simulated backward difference method, *J. met. Soc. Japan*, **44**, pp. 76-84.

Mohanty, U.C., 1982, Some characteristics of dynamic initialization of mass and velocity fields in the lower latitudes, *Mausam*, **33**, pp. 29-33.

Mohanty, U.C. and Madan, S.C., 1985, Certain aspects on the realization of PE forecasting model in the low latitudes, *Mausam*, **36**, pp. 127-134.

Nitta, T., 1969, Initialisation and Analysis for the PE model, Proc. WMO/IUGG Symp. on NWP, Tokyo.

Nitta, T. and Hovermale, J.B., 1969, A technique of objective analysis and initialization for the primitive forecast equations, *Mon. Weath. Rev.*, **97**, pp. 652-658.

Singh, S.S., 1985, Short range prediction with a multi-level primitive equation model, *Proc. Indian Acad. Sci.* (Earth Planet Sci.), **94**, pp. 159-184.

Sugi, Masato, 1986, Dynamical Normal Mode Initialization, Dept. of Met. Florida State University (Unpublishe d).

Temperton, C., 1976, Dynamic initialization for barotropic and multi-level models, *Quart. J.R. met. Soc.*, **102**, pp. 297-311.